# Finite element approximation of a surface-subsurface coupled problem arising in forest dynamics [1]

Gonzalo Galiano [2] and Julián Velasco

*Dpto. de Matemáticas, Universidad de Oviedo, c/ Calvo Sotelo, 33007-Oviedo Spain*

**Abstract**

We propose a finite element approximation for an evolution model describing the spatial population distribution of two salt tolerant plant species, such as mangroves, which are affected by inter- and intra-specific competition (Lotka-Volterra), population pressure (cross-diffusion) and environmental heterogeneity (environmental potential). The environmental potential and the Lotka-Volterra terms are assumed to depend on the salt concentration in the roots region, which may change as a result of mangroves ability for uptaking fresh water and leave the salt of the solution behind, in the saturated porous medium. Consequently, partial differential equations modeling the population dynamics on the surface are coupled with Darcy-transport equations modeling the salt and pressure-velocity distribution in the subsurface. We provide a numerical discretization based on a stabilized mixed finite element method for the transport-Darcy flow problem coupled to a finite element method for a regularized version of the cross-diffusion population model, which we use to numerically demonstrate the behavior of the system.

*Key words:* Population dynamics, cross-diffusion, Darcy flow, stabilized mixed formulation, finite element method.

## 1 Introduction

We present a model for analyzing the spatial distribution evolution of two plant populations which are affected by

[1] Supported by the Spanish MICIIN Project MTM2010-18427

[2] Corresponding author. Phone:+34 985103343 Fax: +34 985103354

[3] galiano@uniovi.es, julian@uniovi.es

- competition for similar resources,
- population pressure, and
- environmental quality.

These conditionings are realized mathematically in the form of a time evolution drift-cross diffusion system of partial differential equations for the biomass densities, $u_i(\bar{x},t) \geq 0$, of species $i=1$ and $i=2$, introduced by Shigesada et al [20]:

$$\partial_t u_i - \operatorname{div} J_i = F_i(\cdot,u_1,u_2), \quad J_i = \nabla(c_i u_i + a_{ii}u_i^2 + a_{ij}u_i u_j) + d_i u_i \nabla\Phi, \quad (1)$$

where $i \neq j$, holding in $S_T = \Gamma_D \times (0,T)$, with $\bar{x} \in \Gamma_D \subset \mathbb{R}^{N-1}$, $N=2$ or 3, open, bounded and with Lipschitz continuous boundary, $\partial\Gamma_D$, and for $t \in (0,T)$ the time, for an arbitrarily fixed $T>0$. The spatial domain $\Gamma_D$ represents the soil surface and is given as the top boundary of an $N-$dimensional bounded set, $\Omega$, the subsurface domain.

The diffusion coefficients $c_i$ and $a_{ij}$ are non-negative constants, and $d_i \in \mathbb{R}$ $(i,j=1,2)$. The source terms are of competitive Lotka-Volterra type

$$F_i(\bar{x},t,u_1,u_2) = \Big(\alpha_i(\bar{x},t) - \beta_{i1}(\bar{x},t)u_1 - \beta_{i2}(\bar{x},t)u_2\Big)u_i, \quad i=1,2, \quad (2)$$

where $\alpha_i \geq 0$ is the intrinsic growth rate of the $i-$specie, $\beta_{ii} \geq 0$ are the coefficients of intra-specific competition, $\beta_{12},\ \beta_{21} \geq 0$ are those of inter-specific competition. Function $\Phi = \Phi(\bar{x},t)$ is the environmental potential, modeling areas where the environmental conditions are more or less favorable [20,18]. We shall describe later how the Lotka-Volterra terms and the environmental potential are related to the evolving environment. The above system of equations is completed with non-flux boundary conditions and initial data:

$$J_i \cdot \nu = 0 \quad \text{on} \quad \partial\Gamma_D \times (0,T), \quad (3)$$
$$u_i(\cdot,0) = u_i^0 \geq 0 \quad \text{on} \quad \Gamma_D, \quad (4)$$

for $i=1,2$, where $\nu$ denotes the exterior unit normal to $\Gamma_D$. We shall refer to problem (1)-(4) as to **Problem $\mathbf{P_S}$**, the surface problem.

This population model has received much attention since its introduction due to the interesting spatial pattern formation that its solutions may exhibit, referred to as *segregation*. Numerical experiments for the evolution problem, see [8,9,3,12], as well as analytical results on the corresponding steady state problem (with $d_i=0$), see [15,16], seem to indicate that while the intensity of diffusion ($c_i$) and self-diffusion ($a_{ii}$) tend to suppress pattern formation, those of cross-diffusion ($a_{12}, a_{21}$) seem to help create segregation patterns. We refer to [22,8,9,5,3,12] and the references therein for analytical results on the existence of solutions and numerical approximations of the problem.

General competitive strategies of populations may include modifying the local environment. A good example is mangrove ecosystems [14], which are tropical communities of tree species typically growing in saline coastal soils. Mangroves are salt tolerant species which are able to exclude most of the salt from the seawater their roots extract from the saturated soil [2]. In this way, they further salinize poorly flushed soils resulting in an increase of their comparative fitness to such areas. As pointed out by Passioura et al [19], differences between species in strategies of water use may affect the spatial distribution of these species: species with high *transpiration rates* [4] may dominate less saline well-flushed habitats while those adapted to low transpiration rates may occupy more saline poorly flushed intertidal areas.

Passioura et al [19] provided an analytical approach to the mechanisms of soil salinization produced by mangroves and investigated the consequences of salt concentration increase on mangroves transpiration rate. Their work was later generalized and extended in a series of papers [6,10,7] from where we recall the following mathematical model. We assume the subsurface region, $\Omega \subset \mathbb{R}^N$, to be an open and bounded set that, after the introduction of dimensionless variables, see [7], takes the form $\Omega = \Gamma_D \times (0,1)$. We denote a point in $\Omega$ by $\mathbf{x} = (\bar{x}, z)$, being $z$ the depth. The subsurface is decomposed into a roots region, $\Omega_d = \Gamma_D \times (0,d)$, $d \in (0,1)$ where a continuous extraction of fresh water takes place, and a region free of roots, $\Omega/\Omega_d$. Let $c \in [0,1]$ be the salt concentration, $\mathbf{q}$ the water flow discharge and $p$ the pressure, and consider the domain $Q_T = \Omega \times (0,T)$, for $T > 0$. The problem reads: Find $c, p : \bar{Q}_T \to \mathbb{R}$ and $\mathbf{q} : \bar{Q}_T \to \mathbb{R}^N$ such that

$$c_t + \mathrm{div}_{\mathbf{x}}(Rc\mathbf{q} - \nabla_{\mathbf{x}} c) = 0, \tag{5}$$
$$\mathrm{div}_{\mathbf{x}}\, \mathbf{q} + g(\cdot, c) = 0, \tag{6}$$
$$\mathbf{q} + \nabla_{\mathbf{x}} p + c\mathbf{e}_z = 0, \tag{7}$$

in $Q_T$. Here, $\mathrm{div}_{\mathbf{x}} = \mathrm{div} + \frac{\partial}{\partial z}$, $\nabla_{\mathbf{x}} = (\nabla, \frac{\partial}{\partial z})$ and the vector $\mathbf{e}_z$ is the canonical vertical vector pointing upwards. Positive parameter $R$ is a Rayleigh number. The usual example considered in the literature [19,7,11] for the extraction function, $g$, is

$$g = g_1 + g_2, \quad g_i(z, c, u_1, u_2) = m_i k_i(z, u_1, u_2)(1-c)_+^{r_i}, \tag{8}$$

for $i = 1, 2$, with $m_i > 0$ the *extraction numbers*, expressing the water uptaking strengths (related to the transpiration rates), $r_i > 0$, and

$$k_i(z, u_1, u_2) = k(z)\frac{u_i}{u_1 + u_2}, \quad \text{with } k(z) = d^{-1} 1_{(0,d)}(z)$$

[4] Transpiration rate is the rate of loss of water vapor from plants surface, taking place mainly from leaves. The amount of water given off depends upon how much water the roots of the plant may absorb.

describing the presence of roots of each specie [21]. In order to prescribe boundary conditions, we decompose the spatial boundary as $\partial\Omega = (\Gamma_D \times \{0\}) \cup \Gamma_N$, with $\Gamma_N = \Big(\Gamma_D \times \{1\}\Big) \cup \Big(\partial\Gamma_D \times (0,1)\Big)$. Here and it what follows, we make the identification $\Gamma_D \equiv \Gamma_D \times \{0\}$. We prescribe

$$c = c_D, \quad p = 0 \quad \text{on } \Gamma_D \times (0,T), \tag{9}$$

$$\nabla_{\mathbf{x}} c \cdot \mathbf{n} = \mathbf{q} \cdot \mathbf{n} = 0 \quad \text{on } \Gamma_N \times (0,T). \tag{10}$$

Finally, the initial distribution

$$c(\cdot, 0) = c_0 \quad \text{in } \Omega, \tag{11}$$

is assumed to satisfy $0 \leq c_0 \leq 1$ in $\Omega$. We shall refer to problem (5)-(7) and (9)-(11) as to **Problem $\mathbf{P_{SS}}$**, the subsurface problem.

Although the environmental potential in equation (1), $\Phi$, is usually assumed to be given, in this model we consider the case in which it depends on the roots zone salt concentration in a way expressing that mangroves populations prefer to establish in regions with low salt concentration. More concretely, we take

$$\Phi(\bar{x}, t) = \int_0^d c(\bar{x}, z, t) dz, \tag{12}$$

where $z = d$ is the roots maximum depth below the surface $\Gamma_D$. In addition, we assume that the Lotka-Volterra coefficients depend on the amount of water that each specie is able to extract (which depends on the salt concentration, $c$) and on other constant coefficients expressing that the species differ both in their ability to exclude salt and in other biological capabilities such as light or nutrients absorption, see [21]. Hence, for

$$G_i(\bar{x}, t; c, u) = \int_0^1 g_i(z, c(\bar{x}, z, t), u(\bar{x}, t)) dz \quad i = 1, 2, \tag{13}$$

where we used the notation $u = (u_1, u_2)$, we define $F_i(\bar{x}, t, u_1, u_2)$ as in (2) with

$$\alpha_i = \alpha_i(G_i(\bar{x}, t; c, u)), \quad \beta_{ij} = \beta_{ij}(G_1(\bar{x}, t; c, u), G_2(\bar{x}, t; c, u)), \tag{14}$$

for some non-negative functions $\alpha_i : \mathbb{R}_+ \to \mathbb{R}_+$ and $\beta_{ij} : \mathbb{R}_+^2 \to \mathbb{R}_+$.

The coupled surface-subsurface problem, which we shall refer to as to **Problem P**, is formed by the surface Problem $\mathrm{P_S}$ with the environmental potential given by (12) and the Lotka-Volterra coefficients given by (14), together with the subsurface Problem $\mathrm{P_{SS}}$ for an extraction function depending on the biomass $u_1$ and $u_2$, e.g. function $g$ defined in (8). To state the result on existence of weak solutions of Problem P obtained in [10] we first introduce the usual concentration and flow-pressure functional spaces corresponding to the

Darcy flow problem:

$$\mathcal{V} = \left\{\eta \in H^1(\Omega) : \eta = 0 \text{ on } \Gamma_D\right\},$$
$$H_{0,N}(\mathrm{div}, \Omega) = \left\{\boldsymbol{\phi} \in L^2(\Omega)^N : \mathrm{div}_{\mathbf{x}}\, \boldsymbol{\phi} \in L^2(\Omega), \boldsymbol{\phi} \cdot \mathbf{n} = 0 \text{ on } \Gamma_N\right\},$$
$$\mathcal{W}_T = \left\{\boldsymbol{\phi} \in L^2(Q_T)^N : \mathrm{div}_{\mathbf{x}}\, \boldsymbol{\phi} \in L^\infty(Q_T)\right\},$$

and the precise assumptions on the data problem:

H$_1$. The spatial domain $\Omega \subset \mathbb{R}^N$, $N \leq 3$ is bounded with a Lipschitz continuous boundary, $\partial\Omega$, which is decomposed as $\partial\Omega = \Gamma_D \cup \Gamma_N$, with $\Gamma_D \cap \Gamma_N = \emptyset$ and with $\Gamma_D$ of positive $N-1$ dimensional measure.

H$_2$. Let $\mathbf{x} = (x, y, z)$, $v = (v_1, v_2)$. The function $g : \bar{Q}_T \times [0,1] \times \mathbb{R}^2 \to \mathbb{R}$ satisfies, for $i = 1, 2$,

$$g(\cdot, \cdot, s, \cdot) \in L^\infty(Q_T \times \mathbb{R}^2) \quad \text{for all } s \in [0,1],$$
$$g(\mathbf{x}, t, \cdot, \cdot) \in C([0,1] \times \mathbb{R}^2) \text{ for a.e. } (\mathbf{x}, t) \in Q_T,$$
$$g(\mathbf{x}, t, \cdot, v) \text{ is non-increasing in } [0,1] \text{ and } g(\mathbf{x}, t, 1, v) = 0 \text{ for a.e. } (\mathbf{x}, t) \in Q_T$$
and for all $v \in \mathbb{R}^2$.

Note that, in particular, $g \geq 0$ in $\bar{\Omega} \times [0,1] \times \mathbb{R}^2$.

H$_3$. The initial and boundary data have the regularity

$$c_0 \in L^\infty(\Omega) \quad \text{and } 0 \leq c_0 \leq 1 \quad \text{a.e. in } \Omega,$$
$$c_D \in H^1(0,T; L^2(\Omega)) \cap L^2(0,T; H^1(\Omega)) \quad \text{and } 0 \leq c_D \leq 1 \quad \text{a.e. in } Q_T,$$
$$u_i^0 \in L_\Psi(\Gamma_D) \quad \text{and } u_i^0 \geq 0 \quad \text{a.e. in } \Gamma_D \ (i = 1, 2),$$

with $L_\Psi(\Gamma_D)$ the Orlicz space for $\Psi(s) = (1+s)\ln(1+s) - s$, see [1].

H$_4$. For $i, j = 1, 2$, $i \neq j$, the constant parameters satisfy $c_i \geq 0$, $a_{ii} > 0$, $a_{ij} \geq 0$, $R \geq 0$, and $m \geq 0$. The Lotka-Volterra coefficients satisfy $\alpha_i \in C^0(\mathbb{R})$, $\beta_{ij} \in C^0(\mathbb{R}^2)$, with $\alpha_i \geq 0$, $\beta_{ii} > \beta > 0$, and $\beta_{12} = \beta_{21} \geq 0$, for some constant $\beta$.

The following theorem was proven in [11].

**Theorem 1** *Let $T > 0$ and assume Hypothesis H$_1$-H$_4$. Then Problem P has a weak solution $(u_1, u_2, c, \mathbf{q}, p)$ satisfying, for $i = 1, 2$, the regularity*

$$u_i \in L^2(0,T; H^1(\Gamma_D)) \cap L^\infty(0,T; L_\Psi(\Gamma_D)) \cap W^{1,r}(0,T; (W^{1,r'}(\Gamma_D))'), \tag{15}$$
$$c \in c_D + L^2(0,T; \mathcal{V}) \cap H^1(0,T; \mathcal{V}') \cap L^\infty(Q_T), \tag{16}$$
$$\mathbf{q} \in L^2(0,T; H_{0,N}(\mathrm{div}, \Omega)) \cap \mathcal{W}_T, \tag{17}$$
$$p \in L^2(0,T; \mathcal{V}), \tag{18}$$

*for* $r = (2N+2)/(2N+1)$ *and* $r' = r/(r-1)$*, and with*

$$u_i \geq 0 \quad \text{in } S_T \quad \text{and} \quad \min\{c_0, c_D\} \leq c \leq 1 \quad \text{in } Q_T.$$

*Equations (1), (5)-(7) are satisfied in the sense*

$$\int_0^T < \partial_t u_i, \varphi >_1 + \int_{S_T} (c_i \nabla u_i + 2a_{ii} u_i \nabla u_i + a_{ij} \nabla(u_i u_j) + d_i u_i \nabla U) \cdot \nabla \varphi$$
$$= \int_{S_T} F_i(\cdot, u_1, u_2)\varphi, \tag{19}$$

*for all* $\varphi \in L^{r'}(0,T; W^{1,r'}(\Gamma_D))$*,* $i \neq j$*, and*

$$< c_t, \eta >_2 - \int_\Omega (Rc\mathbf{q} - \nabla_{\mathbf{x}} c) \cdot \nabla_{\mathbf{x}} \eta = 0, \tag{20}$$
$$\int_\Omega \mathbf{q} \cdot \boldsymbol{\phi} - \int_\Omega p \operatorname{div}_{\mathbf{x}} \boldsymbol{\phi} - \int_\Omega c\mathbf{e}_z \cdot \boldsymbol{\phi} = 0, \tag{21}$$
$$\int_\Omega (\operatorname{div}_{\mathbf{x}} \mathbf{q} + g(\cdot, c, u_1, u_2))\xi = 0, \tag{22}$$

*for all* $\eta \in \mathcal{V}$*,* $\xi \in L^2(\Omega)$*,* $\boldsymbol{\phi} \in H_{0,N}(\operatorname{div}, \Omega)$ *and for a.e.* $t \in (0,T)$*. The notation* $< \cdot, \cdot >_1$ *and* $< \cdot, \cdot >_2$ *stands for the dual products* $W^{1,r'}(\Gamma_D) \times (W^{1,r'}(\Gamma_D))'$ *and* $\mathcal{V}' \times \mathcal{V}$*, respectively. Finally, the initial data* $u_{i,0}$ *and* $c_0$ *are satisfied in the* $L_\Psi$ *and* $L^2$ *senses, respectively.*

## 2 Finite element approximation

Before describing the fully finite element discretization scheme of Problem P let us point out the main difficulties involved in the approximations of Problems $\mathrm{P_{SS}}$ and $\mathrm{P_S}$. On one hand, let us consider the Darcy flow equations of Problem $\mathrm{P_{SS}}$ uncoupled from Problem $\mathrm{P_S}$

$$\operatorname{div}_{\mathbf{x}} \mathbf{q} + g = 0 \qquad \text{in } \Omega, \tag{23}$$
$$\mathbf{q} + \nabla_{\mathbf{x}} p + c\mathbf{e}_{\mathbf{z}} = 0 \qquad \text{in } \Omega, \tag{24}$$
$$\mathbf{q} \cdot \mathbf{n} = 0 \qquad \text{on } \partial\Omega, \tag{25}$$

for some regular functions $g$ and $c$. As it is well known, not all elections of the discrete spaces for the pressure and the velocity satisfy the Babuska-Brezzi stability condition. Indeed, the most natural and simple implementation of continuous piecewise linear functions defined in the same mesh is not stable, see [4]. However, Masud et al [17] introduced an alternative stabilized formulation in which this spaces may be used. The idea is, instead of using the usual

mixed finite element formulation

$$\langle \boldsymbol{\xi}, \mathbf{q} \rangle - \langle \mathrm{div}_{\mathbf{x}}\, \boldsymbol{\xi}, p \rangle + \langle \eta, \mathrm{div}_{\mathbf{x}}\, \mathbf{q} \rangle = - \langle \boldsymbol{\xi}, c\mathbf{e}_z \rangle - \langle \eta, g \rangle \,,$$

for all test functions $\boldsymbol{\xi} \in H(\mathrm{div}, \Omega)$ and $\eta \in L^2(\Omega)$, with $\langle \cdot, \cdot \rangle$ the usual $L^2(\Omega)$ scalar product, consider the following (stabilized) formulation

$$\begin{aligned} \langle \boldsymbol{\xi}, \mathbf{q} \rangle - \langle \mathrm{div}_{\mathbf{x}}\, \boldsymbol{\xi}, p \rangle + \langle \mathrm{div}_{\mathbf{x}}\, \mathbf{q}, \psi \rangle + \frac{1}{2} \langle \mathbf{q} + \nabla_{\mathbf{x}} p, \nabla_{\mathbf{x}} \eta - \boldsymbol{\xi} \rangle \\ = - \langle c\mathbf{e}_z, \boldsymbol{\xi} \rangle - \langle g, \eta \rangle - \frac{1}{2} \langle c\mathbf{e}_z, \nabla_{\mathbf{x}} \eta - \boldsymbol{\xi} \rangle \,, \end{aligned}$$

for all $\boldsymbol{\xi} \in H_{0,N}(\mathrm{div}, \Omega)$ and $\eta \in \mathcal{V}$. In particular, for this stabilized formulation we have that the approximation obtained considering the continuous piecewise lineal spaces in the same mesh for both unknowns verifies the error estimate

$$||\mathbf{q} - \mathbf{q}_h||^2_{L^2(\Omega)^2} + ||\nabla(p - p_h)||^2_{L^2(\Omega)} \leq C_1 |\mathbf{q}|_2 h^2 + C_2 |p|_2 h,$$

where $|\cdot|_2$ is the $2-$th Sobolev seminorm, see [17].

On the other hand, the discretization of Problem $\mathrm{P_S}$ involves other kind of difficulties. A key step of the existence proof of Problem $\mathrm{P_S}$, considered for the following discussion uncoupled from Problem $\mathrm{P_{SS}}$, is to establish and exploit the following entropy inequality, obtained formally when using $\ln(u_i)$ as a test function in the weak formulation of Problem $\mathrm{P_S}$, see [5],

$$\begin{aligned} \frac{d}{dt} \int_{\Gamma_D} \sum_{i=1}^{2} F(u_i) + \int_{\Gamma_D} \sum_{i=1}^{2} (c_i u_i^{-1} + 2a_{ii}) |\nabla u_i|^2 \\ + \int_{\Gamma_D} \sum_{i=1}^{2} |a_{12}(u_2 u_1^{-1})^{1/2} \nabla u_1 + a_{21}(u_1 u_2^{-1})^{1/2} \nabla u_2|^2 \\ = \int_{\Gamma_D} \sum_{i=1}^{2} \Big( - d_i \nabla \Phi \cdot \nabla u_i + F_i(u_1, u_2) F'(u_i) \Big), \end{aligned}$$

with

$$F(s) = s(\ln s - 1) + 1 \geq 0 \quad \text{for all } s \geq 0.$$

Since this estimate is only justified for $u_i > 0$, in the construction of the numerical approximation on has to use a regularization procedure. Barret et al [3] consider the following regularization, $F_\varepsilon \in C^{2,1}(\mathbb{R})$, of $F$:

$$F_\varepsilon(s) = \begin{cases} \frac{s^2 - \varepsilon^2}{2\varepsilon} + (\ln \varepsilon - 1)s + 1 & s \leq \varepsilon, \\ (\ln s - 1)s + 1 & \varepsilon \leq s \leq \varepsilon^{-1}, \\ \frac{\varepsilon(s^2 - \varepsilon^{-2})}{2} + (\ln \varepsilon^{-1} - 1)s + 1 & \varepsilon^{-1} \leq s, \end{cases} \tag{26}$$

for any $\varepsilon > 0$. Then, using the approximation of $\ln u_i$ given by $F'_\varepsilon(u_i)$ as a test function in a correspondingly regularized version of Problem $\mathrm{P_S}$ we obtain the estimates

$$\sup_{t\in(0,T)} \int_{\Gamma_D} \sum_{i=1}^{2} F_\varepsilon(u_{\varepsilon,i}) + \int_0^T \int_{\Gamma_D} \sum_{i=1}^{2} a_{ii} |\nabla u_{\varepsilon,i}|^2 \le C,$$

and

$$\sup_{t\in(0,T)} \int_{\Gamma_D} \sum_{i=1}^{2} |[u_{\varepsilon,i}]_-|^2 \le C\varepsilon,$$

with $[s]_-$ denoting the negative part of $s$. With these estimates one can pass to the limit $\varepsilon \to 0$ to obtain a non-negative weak solution of Problem $\mathrm{P_S}$, see [3], meanwhile for $\varepsilon > 0$ a discrete solution $u_{\varepsilon,i}$ with a small and controlled negative part may be computed.

We now turn to describe the finite element approximation of Problem P. On the set $\Omega$ we consider a family of quasi-uniform partitionings $\left\{\mathcal{T}^h_{SS}\right\}_h$ consisting of disjoint and open simplices $\kappa$ with $h_\kappa = \mathrm{diam}(\kappa)$ and $h = \max_{\kappa\in\mathcal{T}^h_{SS}} h_\kappa$, so that $\bar\Omega = \cup_{\kappa\in\mathcal{T}^h_{SS}} \bar\kappa$. Associated with $\mathcal{T}^h_{SS}$ are the finite element spaces

$$V^h = \left\{ \boldsymbol{\xi} \in H_{0,N}(\mathrm{div},\Omega) \cap C(\bar\Omega)^2 : \boldsymbol{\xi}|_\kappa \quad \text{is linear for all} \quad \kappa \in \mathcal{T}^h_{SS} \right\},$$
$$SS^h = \left\{ \eta \in \mathcal{V} \cap C(\bar\Omega) : \eta|_\kappa \quad \text{is linear for all} \quad \kappa \in \mathcal{T}^h_{SS} \right\}.$$

Similarly, on the interval $\Gamma_D$ we consider the corresponding family of partitionings $\left\{\mathcal{T}^h_S\right\}_h$ given by $I = \kappa \cap \Gamma_D$ with $\kappa \in T^h_{SS}$, $h_I = |I|$ and $h = \max_{I\in\mathcal{T}^h} h_I$, so that $\bar\Gamma_D = \cup_{I\in\mathcal{T}^h_S} \bar I$. Associated with $\mathcal{T}^h_S$ is the finite element space

$$S^h = \left\{ \varphi \in H^1(\Gamma_D) \cap C(\bar\Gamma_D) : \varphi|_I \quad \text{is linear for all} \quad I \in \mathcal{T}^h_S \right\}.$$

Let $J$ be the set of nodes of $\mathcal{T}^h_S$ and $\{p_j\}_{j\in J}$ the coordinates of these nodes. Let $\{\varphi_j\}_{j\in J}$ be the standard basis functions for $S^h$, that is $\varphi_j \in S^h$, $\varphi_j \ge 0$ in $\Gamma_D$, and $\varphi_j(p_i) = \delta_{ij}$ for all $i, j \in J$. In addition to $F_\varepsilon$ given by (26), the following functions were introduced in [3], see also [13,23], to control the possible negativity of discrete approximate solutions. For $\varepsilon > 0$, we define $\lambda_\varepsilon : \mathbb{R} \to \mathbb{R}$ as $\lambda_\varepsilon(s) = (F''_\varepsilon(s))^{-1}$, and $\Lambda_\varepsilon : S^h \to L^\infty(\Omega)$ as

$$\Lambda_\varepsilon(z^h)|_I = \begin{cases} \frac{z^h(p_k) - z^h(p_j)}{F'_\varepsilon(z^h(p_k)) - F'_\varepsilon(z^h(p_j))} & z^h(p_k) \ne z^h(p_j), \\ \lambda_\varepsilon(z^h(p_k)) & z^h(p_k) = z^h(p_j). \end{cases}$$

Observe that we always have $\Lambda_\varepsilon(z^h)|_\kappa = \lambda_\varepsilon(z^h(\xi))$ for some $\xi \in I$ and $\lambda_\varepsilon(s) \to s1_{[0,\infty)}(s)$ as $\varepsilon \to 0$.

For the time discretization, we consider a partitioning $0 = t_0 < t_1 < \ldots < t_{K-1} < T_K = T$ of $[0,T]$ into possibly variable time steps $\tau_k = t_k - t_{k-1}$,

$k = 1, \ldots, K$, and set $\tau = \max_k \tau_k$. We now assume, for simplicity, that the concentration boundary data is $c_D = 0$. To treat the general case, we just would introduce the new unknown $\hat{c} = c - c_D$, and perform the corresponding substitution. For any given $\varepsilon \in (0,1)$ let $c_\varepsilon^{k-1} \in SS^h$, $u_{\varepsilon,i}^{k-1} \in S^h$, $i = 1,2$ be given approximations of a solution of Problem P for time $t_{k-1}$. For $k = 1$ we define $c_\varepsilon^0$ and $u_{\varepsilon,i}^0$ to be the $L^2$ projections of $c_0$ and $u_i^0$ on $SS^h$ and $S^h$, respectively. We then consider the following stabilized mixed finite element approximation of Problem $\mathrm{P}_{SS}$: For $k \geq 1$ find $\mathbf{q}_\varepsilon^k \in \mathcal{V}^h$ and $p_\varepsilon^k, c_\varepsilon^k \in SS^h$ such that for all $\boldsymbol{\xi} \in \mathcal{V}^h$ and all $\eta \in SS^h$,

$$\begin{aligned}\left\langle \mathbf{q}_\varepsilon^k, \boldsymbol{\xi}, \right\rangle - \left\langle p_\varepsilon^k, \mathrm{div}_{\mathbf{x}}\, \boldsymbol{\xi} \right\rangle + \left\langle \mathrm{div}_{\mathbf{x}}\, \mathbf{q}_\varepsilon^k, \eta \right\rangle \\ + \frac{1}{2}\left\langle \mathbf{q}_\varepsilon^k + \nabla_{\mathbf{x}} p_\varepsilon^k, \nabla_{\mathbf{x}}\eta - \boldsymbol{\xi} \right\rangle = -\left\langle c_\varepsilon^k \mathbf{e}_z, \boldsymbol{\xi} \right\rangle \\ - \left\langle g(\cdot, c_\varepsilon^k, u_{\varepsilon,1}^{k-1}, u_{\varepsilon,2}^{k-1}), \eta \right\rangle - \frac{1}{2}\left\langle c_\varepsilon^k \mathbf{e}_z, \nabla_{\mathbf{x}}\eta - \boldsymbol{\xi}) \right\rangle, \quad (27)\end{aligned}$$

and, for all $\phi \in SS^h$,

$$\frac{1}{\tau_k}\left\langle c_\varepsilon^k - c_\varepsilon^{k-1}, \phi \right\rangle + \left\langle \nabla_{\mathbf{x}} c_\varepsilon^k, \nabla_{\mathbf{x}}\phi \right\rangle = R\left\langle -\mathbf{q}_\varepsilon^k \cdot \nabla_{\mathbf{x}} c_\varepsilon^k + c_\varepsilon^k g(\cdot, c_\varepsilon^k, u_{\varepsilon,1}^{k-1}, u_{\varepsilon,2}^{k-1}), \phi \right\rangle. \quad (28)$$

Then, once we have an approximation $c_\varepsilon^k$ for time $t_k$, we consider the following finite element approximation of Problem $\mathrm{P_S}$: find $(u_{\varepsilon,1}^k, u_{\varepsilon,2}^k) \in (S^h)^2$ such that for $i, j = 1, 2$, with $j \neq i$, and for all $\varphi \in S^h$

$$\begin{aligned}\frac{1}{\tau_k}\left\langle u_{\varepsilon,i}^k - u_{\varepsilon,i}^{k-1}, \varphi \right\rangle + \left\langle \left[c_i + 2a_{ii}\Lambda_\varepsilon(u_{\varepsilon,i}^k) + a_{ij}\Lambda_\varepsilon(u_{\varepsilon,j}^k)\right]\nabla u_{\varepsilon,i}^k, \nabla\varphi \right\rangle \\ + \left\langle \Lambda_\varepsilon(u_{\varepsilon,i}^k)\left[a_{ij}\nabla u_{\varepsilon,j}^k + d_i \nabla \Phi_\varepsilon^k\right], \nabla\varphi \right\rangle \\ = \left\langle u_{\varepsilon,i}^k \left[\alpha_{\varepsilon,i}^{k-1} - \beta_{\varepsilon,i1}^{k-1}\lambda_\varepsilon(u_{\varepsilon,1}^{k-1}) - \beta_{\varepsilon,i2}^{k-1}\lambda_\varepsilon(u_{\varepsilon,2}^{k-1}))\right], \varphi \right\rangle. \quad (29)\end{aligned}$$

Here, $\Phi_\varepsilon^k$ is determined through relation (12) with $c$ replaced by $c_\varepsilon^k$. Similarly are defined the coefficients $\alpha_{\varepsilon,i}^{k-1}$ and $\beta_{\varepsilon,ij}^{k-1}$ from relations (13)-(14).

We finish this section with the following observations on the well-possedness of the finite element approximation. On one hand, as shown in Theorem 2.1 of [3], Problem (29) (for an uncoupled version of Problem $\mathrm{P_S}$) admits a solution. More concretely, if $(u_{\varepsilon,1}^{n-1}, u_{\varepsilon,2}^{n-1}) \in (S^h)^2$, $\varepsilon \in (0, e^{-2})$ and $\tau_n \leq \omega^{-1}$, with

$$\omega = \max\{2\alpha_1 + \beta_{11} + \beta_{12}, 2\alpha_2 + \beta_{21} + \beta_{22}\}$$

then there exists a solution $(u_{\varepsilon,1}^n, u_{\varepsilon,2}^n) \in (S^h)^2$ to the k-th step of Problem (29). In addition, they prove (Theorem 3.1 of [3]) that if $\tau \to 0$ with either $\tau_1 \leq Ch^2$ or $u_i^0 \in H^1(\Omega)$, and if $\varepsilon h^{-1/2} \to 0$ then a subsequence (not relabeled) of

$$u_{\varepsilon,i}(t) = \frac{t - t_{n-1}}{\tau_n} u_{\varepsilon,i}^n + \frac{t_n - t}{\tau_n} u_{\varepsilon,i}^{n-1} \quad t \in [t_{n-1}, t_n], \quad n \geq 1,$$

may be extracted such that $(u_{\varepsilon,1}, u_{\varepsilon,2}) \to (u_1, u_2)$ in a suitable sense, being $(u_1, u_2)$ a weak solution of Problem $\mathrm{P_S}$. On the other hand, we are not aware of a similar result for the transport-Darcy flow problem, Problem $\mathrm{P_{SS}}$. However, the existence proof of [11] is based in uncoupling the Problem P in a similar way than the scheme (27)-(29) and a subsequent coupling of the problem by a fixed point argument in which the actual implementation of the finite element approach is carried out, see (32)-(35).

## 3 Numerical experiments

Before presenting some numerical experiments in space dimension $N = 2$, i.e., $\Omega \subset \mathbb{R}^2$ (a square, in the simulations) and $\Gamma \subset \mathbb{R}$, an open interval, we state briefly our fixed point type algorithms for solving the resulting system of nonlinear algebraic equations for $\mathbf{q}_\varepsilon^k, p_\varepsilon^k, c_\varepsilon^k, u_{\varepsilon,i}^k$ arising at each time level from the approximation (27)-(29). We used the following iterative approach: Given $c_\varepsilon^{k,0}, u_{\varepsilon,i}^{k,0}$, $i = 1, 2$, for $l \geq 1$, find $\mathbf{q}_\varepsilon^{k,l} \in \mathcal{V}^h$, $p_\varepsilon^{k,l}, c_\varepsilon^{k,l} \in SS^h$ and $u_{\varepsilon,i}^{k,l} \in S^h$, such that for $i = 1, 2$ and for all $\boldsymbol{\xi} \in \mathcal{V}^h$, $\eta, \phi \in SS^h$ and $\varphi \in S^h$ we have

$$\left\langle \mathbf{q}_\varepsilon^{k,l}, \boldsymbol{\xi}, \right\rangle - \left\langle p_\varepsilon^{k,l}, \mathrm{div}_{\mathbf{x}}\, \boldsymbol{\xi} \right\rangle + \left\langle \mathrm{div}_{\mathbf{x}}\, \mathbf{q}_\varepsilon^{k,l}, \eta \right\rangle \tag{30}$$

$$+ \frac{1}{2} \left\langle \mathbf{q}_\varepsilon^{k,l} + \nabla_{\mathbf{x}} p_\varepsilon^{k,l}, \nabla_{\mathbf{x}} \eta - \boldsymbol{\xi} \right\rangle = - \left\langle c_\varepsilon^{k,l-1} \mathbf{e}_z, \boldsymbol{\xi} \right\rangle \tag{31}$$

$$- \left\langle g(\cdot, c_\varepsilon^{k,l-1}, u_{\varepsilon,1}^{k-1}, u_{\varepsilon,2}^{k-1}), \eta \right\rangle - \frac{1}{2} \left\langle c_\varepsilon^{k,l-1} \mathbf{e}_z, \nabla_{\mathbf{x}} \eta - \boldsymbol{\xi}) \right\rangle, \tag{32}$$

$$\frac{1}{\tau_k} \left\langle c_\varepsilon^{k,l} - c_\varepsilon^{k-1}, \phi \right\rangle + \left\langle \nabla_{\mathbf{x}} c_\varepsilon^{k,l}, \nabla_{\mathbf{x}} \phi \right\rangle = \tag{33}$$

$$R \left\langle -\mathbf{q}_\varepsilon^{k,l} \cdot \nabla_{\mathbf{x}} c_\varepsilon^{k,l-1} + c_\varepsilon^{k,l-1} g(\cdot, c_\varepsilon^{k,l-1}, u_{\varepsilon,1}^{k-1}, u_{\varepsilon,2}^{k-1}), \phi \right\rangle, \tag{34}$$

and

$$\begin{aligned} &\frac{1}{\tau_k} \left\langle u_{\varepsilon,i}^{k,l} - u_{\varepsilon,i}^{k-1}, \varphi \right\rangle + \left\langle \Big[ c_i + 2a_{ii} \Lambda_\varepsilon(u_{\varepsilon,i}^{k,l-1}) + a_{ij} \Lambda_\varepsilon(u_{\varepsilon,j}^{k,l-1}) \Big] \nabla u_{\varepsilon,i}^k, \nabla \varphi \right\rangle \\ &\quad + \left\langle \Lambda_\varepsilon(u_{\varepsilon,i}^{k,l-1}) \Big[ a_{ij} \nabla u_{\varepsilon,j}^{k,l-1} + d_i \nabla \Phi_\varepsilon^{k,l-1} \Big], \nabla \varphi \right\rangle \\ &\quad = \left\langle u_{\varepsilon,i}^{k,l-1} \Big[ \alpha_{\varepsilon,i}^{k-1} - \beta_{\varepsilon,i1}^{k-1} \lambda_\varepsilon(u_{\varepsilon,1}^{k-1}) - \beta_{\varepsilon,i2}^{k-1} \lambda_\varepsilon(u_{\varepsilon,2}^{k-1})) \Big], \varphi \right\rangle. \end{aligned} \tag{35}$$

We set, for $k \geq 1$, $c_\varepsilon^{k,0} = c_\varepsilon^{k-1}$ and $u_{\varepsilon,i}^{k,0} = u_{\varepsilon,i}^{k-1}$ and adopt the stopping criteria

$$\max_{i=1,2} \Big\{ \|c^{k,l} - c^{k,l-1}\|_\infty, \|u_i^{k,l} - u_i^{k,l-1}\|_\infty \Big\} < \mathrm{tol},$$

with $\mathrm{tol} = 10^{-7}$ in the experiments, and set $\mathbf{q}_\varepsilon^k = \mathbf{q}_\varepsilon^{k,l}$, $p_\varepsilon^k = p_\varepsilon^{k,l}$, $c_\varepsilon^k = c_\varepsilon^{k,l}$ and $u_{\varepsilon,i}^{k-1} = u_{\varepsilon,i}^{k,l}$. Although there is not a proof of the convergence of the iteration (32)-(35), we observed good convergence properties in practice. In

all experiments we integrated in time until a numerical stationary solution, $u_i^S$, was achieved. This was determined by

$$\max_{i=1,2} \left\{ \|c^{k,1} - c^{k,0}\|_\infty, \|u_i^{k,1} - u_i^{k,0}\|_\infty \right\} < 5 \times 10^{-12}.$$

### *3.1 Experiments*

We consider the spatial domain $\Omega = (0,4) \times (0,1)$, which is discretized by a triangular finite elements mesh containing 900 nodes. The top spatial boundary $\Gamma_D = (0,4) \times \{0\}$ contains 30 nodes. The time step is selected considering the main time scales of the problem i.e., diffusion and convection. We take $dt = \min\{0.5\ dx^{-2}, (R\ dx)^{-1}\}$, with $dx = 1/30$. In some situations, for instance when large gradients of populations density arise, we interpolate the data of Problem $\mathrm{P}_S$ to a finer mesh on $\Gamma_D$ in order to get a smoother approximation. The data on Table 1 is common for all the experiments. Observe that the linear diffusions are set to zero, and that the cross-diffusion coefficients have the same value, indicating that population pressures affect in a similar way to both species. The differences between the biological characteristics of the species (mangroves represented by $u_1$ and a less salt tolerant specie represented by $u_2$) are captured by (i) the convection coefficients, $d_1 \ll d_2$, indicating a bigger attraction of Specie 2 than mangroves towards the low salinity areas, and (ii) the coefficients appearing in the extraction function, $g$, i.e., the extraction numbers, $m_1 < m_2$, indicating a more efficient behaviour of Specie 2 for extracting water when no salt is present, and $r_1 < 1 < r_2$, implying a larger capacity of mangroves to uptake fresh water from saline waters. Since we take a relatively low Rayleigh number we do not expect neither large gradients of the salt concentration nor important variations of the flow in the subsurface. However, the situation changes on the surface due to the powerful combination of the drift effects produced by the environmental potential and the repulsive effects of the cross-diffusion. This combination results on large gradients of the populations density in the "good" environmental regions.

**Experiment 1.** We test the model in a standard situation. We take the salt concentration data as $c_0 = c_D = 0.5$, and initial population distributions which contain areas where the species are isolated and areas where the species share the space with equal population density, see Fig. 1. We set the Lotka-Volterra terms to zero, implying for the continuous model that the populations mass have to be conserved. Indeed, for the discrete model, recalling that the time discretization scheme is explicit, the mass conservation property is quite well captured, having a relative error of the order of $10^{-5}$. More precisely, for the

Table 1
Parameter values common for all the experiments

| Parameter | Symbol | Value |
|---|---|---|
| Diffusion coefficients | $c_1, c_2$ | 0 |
| Cross and self diff. coeff. | $a_{ij}$ | 0.1 |
| Convection coefficients | $d_1, d_2$ | $1, 40$ |
| Rayleigh number | $R$ | 100 |
| Extraction coefficients | $m_1, m_2$ | $0.05, 0.1$ |
| Extraction powers | $r_1, r_2$ | $0.5, 2$ |
| Roots depth | $d$ | 0.25 |

stopping time $T = 80$ years (dimensional model), we have

$$\max_{i=1,2}\left\{\Big(\int_0^4 u_{i0}(x)dx - \int_0^4 u_i(x,T)dx\Big)\Big(\int_0^4 u_{i0}(x,t)dx\Big)^{-1}\right\} = 1.3794\times 10^{-5}.$$

In Fig. 1 we show the initial and final population density distributions for both species. Since the initial salt concentration distribution is homogeneous, the environmental potential is initially not attracting the populations to a definite place. However, as time evolves, mangroves salinize the region they occupy, creating a gradient on the environmental potential which drives the population of Specie 2 rapidly ($40 = d_2 \gg d_1 = 1$) towards the potential minimum. Fig. 2 shows the population distributions evolution by plotting $u_i(x,t)$ for $t = 0,\ 15,\ 30,\ 45,\ 60,\ 80$ years. In Figs. 3 and 4 we show some aspects of the concentration-flow problem in the porous medium: the evolution of the environmental potential (same time slices than above), given by

$$U(x,t) = \int_0^{0.25} c(x,z,t)dz,$$

the water flow, and two time slices of the salt concentration. Observe that the absolute changes of the environmental potential are very small, but enough to induce the populations segregation.

**Experiment 2.** We use the same initial population distributions than in Experiment 1 but assume an initial and boundary salt concentration which increases with $x$, simulating a usual situation in the mangroves habitats near the shore, see Fig. 6, left. We again set the Lotka-Volterra terms to zero. We run the program till $T = 80$ years and check that the relative error for the populations mass conservation is of the order $10^{-16}$. In Fig. 5 we show the population distributions evolution by plotting $u_i(x,t)$ for $t = 0,\ 15,\ 30,\ 45,\ 60,\ 80$ years. The drift effect is notorious for Specie 2. In Fig. 6, right, we plot the salt concentration distribution for $T = 80$ years and $z = 0,\ 0.25,\ 1$, i.e., on

the surface, at the lower limit of the roots region, and on the bottom. We observe that, although increasing faster than in other regions, the boundary $x = 0$ keeps being an attraction point region (lower salt concentration) where population of Specie 2 tends to concentrate.

In the following two experiments we explore the effects of the competition terms. We take initial population distributions constant and equal, $u_{10} = u_{20} = 0.5$, and keep the initial salt concentration as in Experiment 2.

**Experiment 3.** We consider two sets of Lotka-Volterra terms in order to compare the evolution of population densities for fixed and varying growth and competition coefficients. More explicitly, we take, for $i = 1, 2$,

$$F_1(x,t) = G_1(x,t)\Big(300 - 100u_1(x,t) - 50u_2(x,t)\Big)u_1(x,t),$$
$$F_2(x,t) = G_2(x,t)\Big(300 - 50u_1(x,t) - 100u_2(x,t)\Big)u_2(x,t),$$

with $G_i$ given by

$$G_i(x,t) = m_i \frac{u_i(x,t)}{u_1(x,t) + u_2(x,t)} \int_0^d (1 - c(x,z,t))_+^{r_i} dz,$$

and similar functions $\tilde{F}_i$ with $G_i(x,t)$ replaced by the constant value

$$\tilde{G}_i = \frac{1}{4}\int_0^4 G_i(x,0)dx.$$

We denote by $\tilde{u}_i$ the solutions corresponding to $\tilde{F}_i$ (Problem $\tilde{\mathrm{P}}$) . We observe that, although the Lotka-Volterra coefficients would give a coexistence state for the corresponding dynamical system, in both cases (Problems P and $\tilde{\mathrm{P}}$) the system seems to converge to the extinction of Specie2, $u_2 = \tilde{u}_2 = 0$, and to the equilibrium value $u_1 = \tilde{u}_1 = 3$ for the mangroves population. However, although qualitatively similar, the solutions of both problems have important quantitative differences. In Fig. 7, left, we plot the relative differences $\|u_i - \tilde{u}_i\|_{L^2(\Gamma_D)}\|\tilde{u}_i\|^{-1}_{L^2(\Gamma_D)}$. The magnitude of the difference is well explained by the time evolution of the coefficients of Problem P, which are captured by the extraction functions $G_i$, in comparison with the constant coefficients of Problem $\tilde{\mathrm{P}}$. We plot in Fig. 7, center, the space average of these functions, i.e.,

$$\frac{1}{4}\int_0^4 G_i(x,t)dx.$$

Another visualization of the quantitative differences between the tho sets of solutions is given in Fig. 7, right, where we plot the space averaged mass populations

$$U_i(t) = \frac{1}{4}\int_0^4 u_i(x,t)dx, \quad \tilde{U}_i(t) = \frac{1}{4}\int_0^4 \tilde{u}_i(x,t)dx,$$

and the semi-total mass populations $(U_1 + U_2)/2$, and $(\tilde{U}_1 + \tilde{U}_2)/2$. We see that after a transient state of about one hundred years, both systems enter in a phase of slow increase (decrease) of the mass of mangroves (Specie2). However, the quantitative differences between both problems are significant. Mangrove (Specie 2) population is always larger (smaller) for Problem P than for Problem $\tilde{\mathrm{P}}$. We also observe that the mass of Specie 2 corresponding to the constant coefficients, $\tilde{u}_2$, is always above the initial mass, whereas the same quantity for the variable coefficients problem drops below the initial state after some 150 years. It is also interesting to notice that the total mass is practically constant for both problems, after the transient state.

Finally, in Fig. 8 we plot time slices showing the evolution of the populations distributions for problems P and $\tilde{\mathrm{P}}$. We see that after a fast initial growth of Specie 2, its population declines and tends to disappear from the *bad* environmental region. This effect is specially visible for solutions of Problem P. In fact, the competition between both populations seems to be more extreme in the case of variable coefficients, as may be seen in the *good* region boundary $x = 0$. The evolution of the system seems to lead to the semi-trivial steady state $(u_1, u_2) = (3, 0)$, i.e. extinction of Specie 2.

## References


[1] R. A. Adams, Sobolev Spaces, Academic Press, New York, 1975.

[2] M. C. Ball, Salinity tolerance in the mangroves *Aegiceras corniculatum* and *Avicennia marina*. I. Water use in relation to growth, carbon partitioning and salt balance, Aust. J. Plant Physiol. 15 (1988) 447-464.

[3] J. W. Barrett, J. F. Blowey, Finite element approximation of a nonlinear cross-diffusion population model, Numer. Math. 98 (2004) 195221.

[4] F. Brezzi, M. Fortin, Mixed and hybrid finite element methods, Springer Series in Computational Mathematics, 15, Springer-Verlag, New York, 1991.

[5] L. Chen, A. Jüngel, Analysis of a multidimensional parabolic population model with strong cross-diffusion, SIAM J. Math. Anal. 36(1) (2004), 301–322.

[6] C. J. van Duijn, G. Galiano, M. A. Peletier, A diffusion-convection problem with drainage arising in the ecology of mangroves, Interfaces and Free Boundaries 3 (2001) 15-44.

[7] C. J. van Duijn, G. Galiano, J. Velasco, Existence of solutions and stability analysis for a Darcy flow with extraction. Nonlinear Analalysis RWA 10(4) (2009) 2007-2020.

[8] G. Galiano, M. L. Garzón, A. Jüngel, Analysis and numerical solution of a nonlinear cross-diffusion system arising in population dynamics, RACSAM Rev. R. Acad. Cienc. Exactas Fs. Nat. Ser. A Mat. 95(2) (2001), 281-295

[9] G. Galiano, M. L. Garzón, A. Jüngel, Semi-discretization in time and numerical convergence of solutions of a nonlinear cross-diffusion population model, Numer. Math. 93(4) (2003) 655-673.

[10] G. Galiano, J. Velasco, On a dynamical boundary value problem arising in the ecology of mangroves. Nonlinear Analysis RWA 7(5) (2006) 1129-1144.

[11] G. Galiano, J. Velasco, Competing through altering the environment: A cross-diffusion population odel coupled to transport-Darcy flow equations. Nonlinear Analysis RWA 12 (2011) 2826-2838.

[12] G. Gambino, M.C. Lombardo, M. Sammartino, A velocitydiffusion method for a LotkaVolterra system with nonlinear cross and self-diffusion, Applied Numerical Mathematics 59 (2009) 1059-1074.

[13] G. Grün, M. Rumpf, Nonnegativity preserving convergent schemes for the thin film equation, Numer. Math. 87 (2000) 113-152.

[14] P. Hutchings, P. Saenger, Ecology of mangroves, Queensland, University of Queensland Press, 1987.

[15] Y. Lou, W.-M. Ni, Diffusion, self-diffusion and cross-diffusion, J. Diff. Eqs. 131 (1996), 79-131.

[16] Y. Lou, W.-M. Ni, Y. Wu, The global existence of solutions for a cross-diffusion system, Adv. Math., Beijing 25 (1996), 283-284.

[17] A. Masud, T. Huges, A stabilized mixed finite element method for Darcy flow, Computer methods in applied mechanics and engineering 191 (2002), 4341-4370.

[18] M. Mimura, K. Kawasaki, Spatial segregation in competitive interaction-diffusion equations, J. Math. Biol. 9 (1980) 49-64.

[19] J. B. Passioura, M. C Ball, J. H. Knight, Mangroves may salinize the soil and in so doing limit their transpiration rate, Funct. Ecol. 6 (1992) 476-481.

[20] N. Shigesada, K. Kawasaki, E. Teramoto, Spatial segregation of interacting species, J. Theor. Biol. 79 (1979), 83-99.

[21] S. Y. Teh, D. L. DeAngelis, L. S. Lobo Sternberg, F. R. Miralles-Wilheim, T. J. Smith, H. L. Koh, A simulation model for projecting changes in salinity concentrations and species dominance in the coastal margin habitats of the Everglades, Ecological Modelling 213 (2008) 245-256.

[22] A. Yagi, Global solution to some quasilinear parabolic system in population dynamics, Nonlinear Analysis TMA 21 (1993), 603-630.

[23] L. Zhornitskaya, A. L. Bertozzi, Positivity-preserving numerical schemes for lubrication-type equations, SIAM J. Numer. Anal. 37(2) (2000), 523-555.

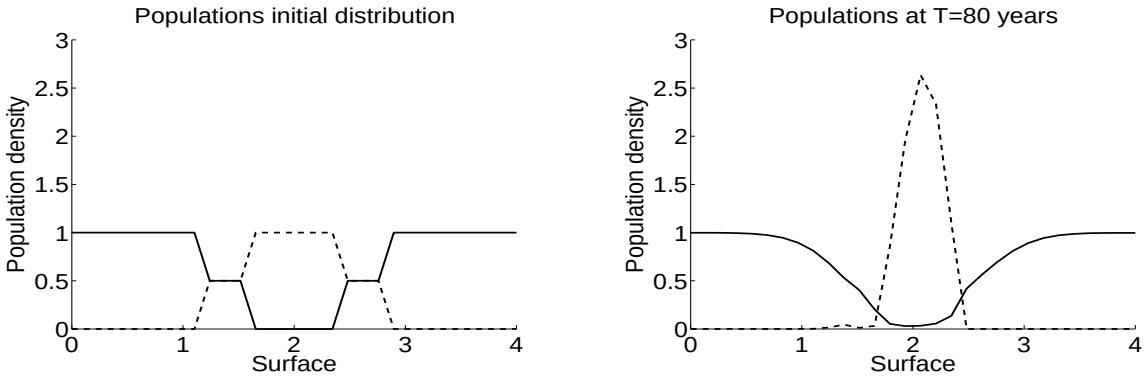


Fig. 1. Experiment 1. Continuous line: mangroves. Dotted line: Specie 2.

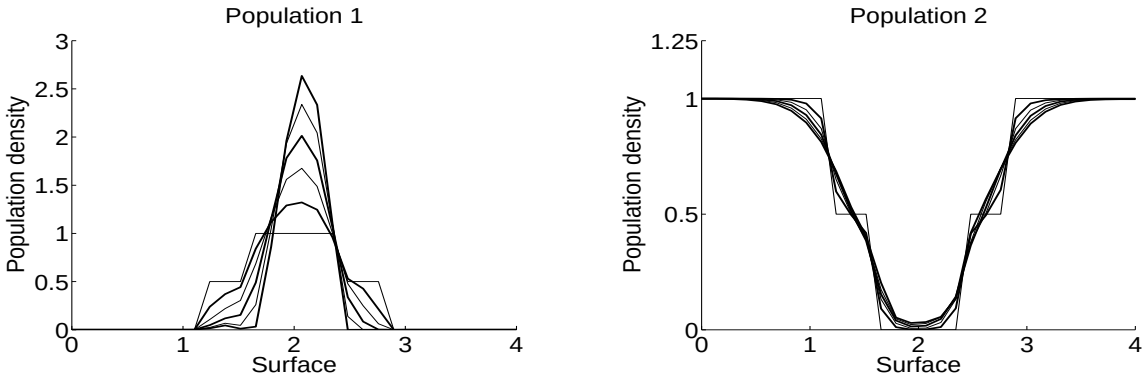


Fig. 2. Experiment 1. Time slices of the evolution of Specie 2 (left) and mangroves (right).

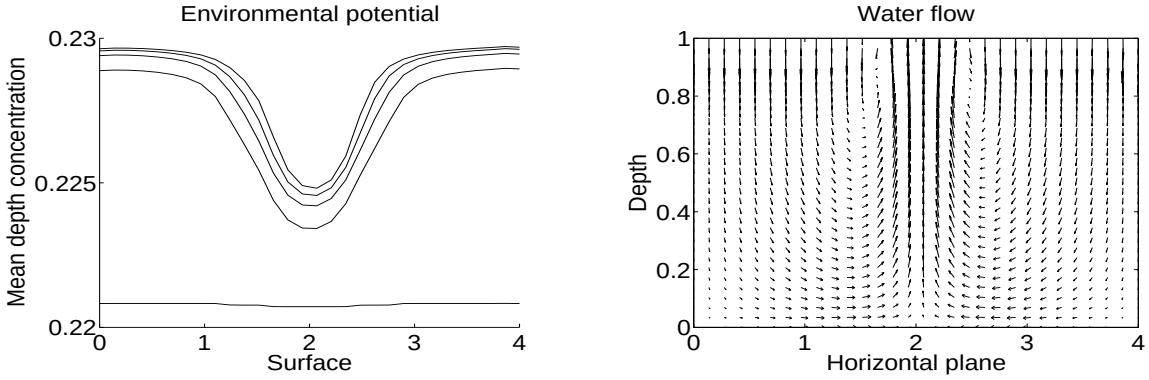


(a) Time slices of the evolution of the environmental potential.

(b) Water flow in the porous medium for T=80 years.

Fig. 3. Experiment 1. In the subsurface.

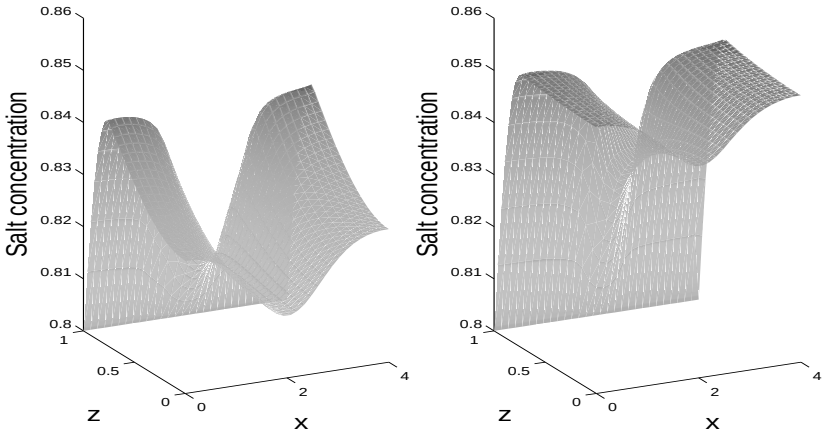


Fig. 4. Experiment 1. Salt concentration in the porous medium for T=10 years (left) and T=80 years (right). $z = 1$ corresponds to the top boundary $\Gamma_D$.

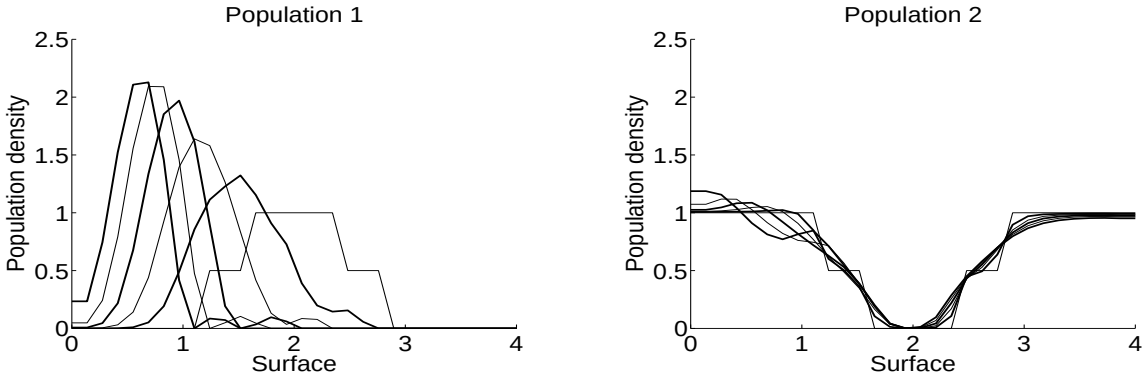


Fig. 5. Experiment 2. Time slices of the evolution of Specie 2 (left) and mangroves (right).

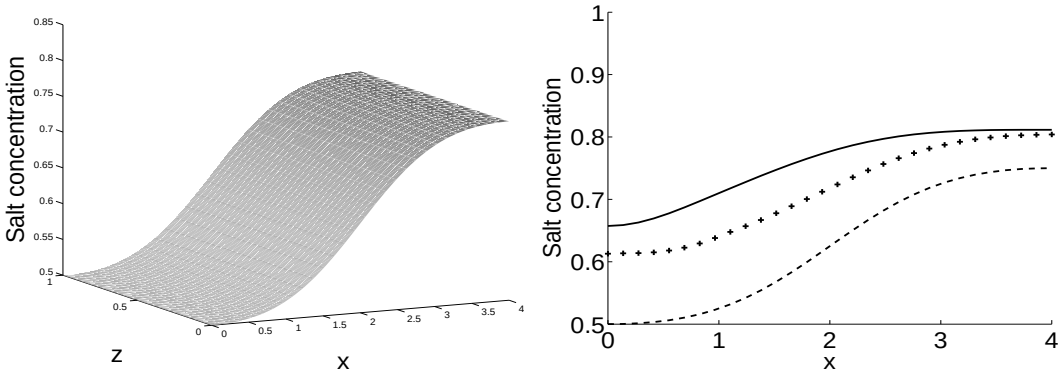


Fig. 6. Experiment 2. Salt concentration in the soil. Left: for $T = 0$. Right: for $T = 80$ years and at the bottom, $z = 1$, (continuous line), lower limit of the roots region, $z = 0.25$, (crossed line) and surface $z = 0$ (dotted line).

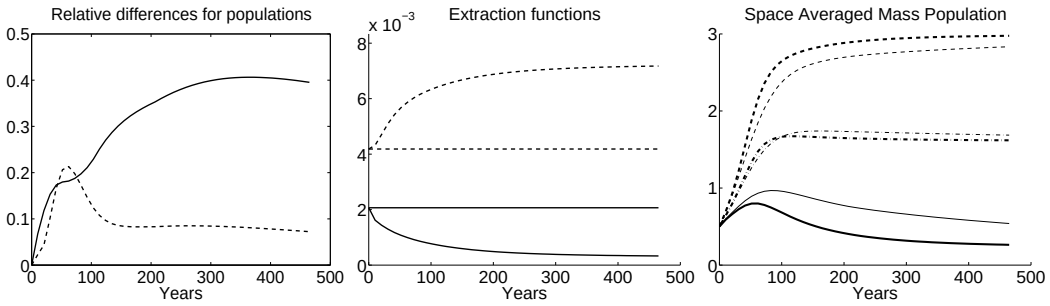


Fig. 7. Experiment 3. Several visualizations of the differences among solutions of Problems P and $\tilde{\text{P}}$. Mangroves: dotted lines, Specie 2: continuous lines.

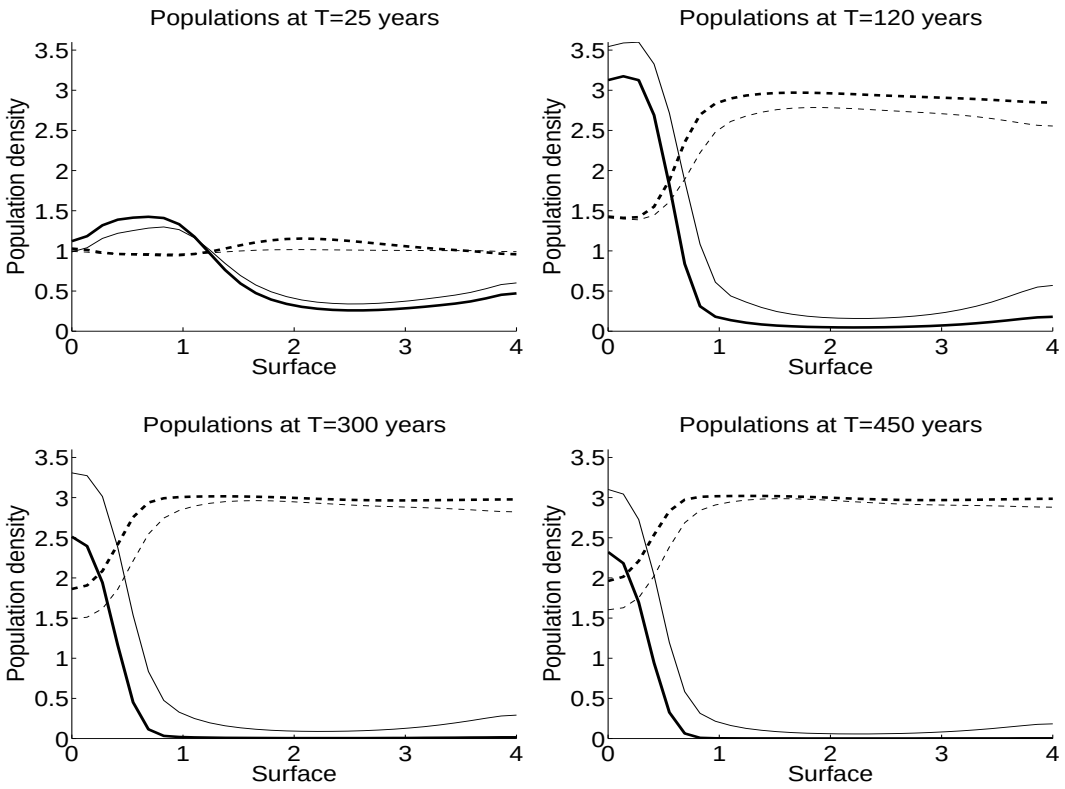


Fig. 8. Experiment 3. Populations evolution. Mangroves: dotted lines, Specie 2: continuous lines. Problem P: thick lines. Problem $\tilde{\text{P}}$: thin lines.